JOURNAL OF THE ELECTROCHEMICAL SOCIETY

ELECTROCHEMICAL SCIENCE AND TECHNOLOGY

SEPTEMBER 1990

The Lead Anode in Alkaline Solutions

III. Growth of Thick PbO Films

V. I. Birss and M. T. Shevalier[1]

Department of Chemistry, University of Calgary, Calgary, Alberta, Canada T2N 1N4

ABSTRACT

The mechanism of formation of thick, porous, PbO films at a Pb anode in 1*N* NaOH solutions was investigated. Film growth initiates by a nucleation process and then proceeds at a rate which is controlled by the increasing resistance of the solution in the narrowing pores of the oxide film. The observed *i/E* relationships were simulated on the basis of two models of film growth, one involving the spreading of islands of film of constant height, and the other in which nuclei both spread and increase in height until the electrode surface is almost fully covered. The latter model led to a very good fit between the observed and calculated curves.

Of the two common forms of lead oxide, PbO and PbO_2, the electrochemistry of the tetravalent oxide has been studied in greater detail, particularly in acid solutions, due to its central role in the Pb/acid storage battery (1-3). In comparison, little has been reported about the electrochemical behavior of PbO in either acidic or basic solutions, despite the numerous applications of PbO in such areas as the glass and ceramics industry, in the production of Pb-containing pigments, in pesticides, soaps, plates, in storage batteries, etc. (4, 5).

Of the published work regarding PbO electrochemistry, most has been based on the results of galvanostatic studies (6-11). More recently, a photoelectrochemical study of PbO and PbO_2 films, formed by the potentiodynamic sweep method in *p*H 9 solutions, has been published (12).

In the last few years, we have been carrying out a detailed study of the electrochemical behavior of Pb in alkaline solutions, focusing primarily on *p*H 14 solutions (13, 14). It has been shown (13) that the first step in the oxidation of Pb at *p*H 14 is the formation of a small amount of a $Pb(OH)_2$ film on the Pb electrode surface (reactions [1]-[3]). With the use of cyclic voltammetry, steady-state and transient potentiostatic methods, as well as rotating disk electrode techniques, it was found that the $Pb(OH)_2$ film readily dissolves as $Pb(OH)_3^-$ (reaction [3]). $Pb(OH)_2$ can also undergo a dehydration process (reaction [4]) according to the following reaction scheme

$$Pb + OH^- \rightleftharpoons (PbOH)_{ads} + e^- \quad [1]$$

$$(PbOH)_{ads} + OH^- \rightleftharpoons Pb(OH)_2 + e^- \quad [2]$$

$$Pb(OH)_2 + OH^- \rightleftharpoons Pb(OH)_3^- \quad [3]$$

$$Pb(OH)_2 \rightleftharpoons PbO + H_2O \quad [4]$$

These reactions occur in the range of potential from about 200 to 300 mV *vs.* RHE, with reaction [3] being the rate-determining step. The occurrence of reactions [1]-[4] is consistent with the prior suggestions in the literature regarding the early stages of Pb oxidation in alkaline solutions (6-11).

At potentials more positive than about 300 mV *vs.* RHE, cyclic voltammetric and chronoamperometric experiments have revealed that a PbO film forms directly on the Pb electrode surface by an instantaneous three-dimensional nucleation and growth mechanism, under diffusion control (14). Reactions [5]-[7] reflect PbO film growth under these conditions, with reaction [6] considered to be the rate-determining step under steady-state conditions

$$Pb + OH^- \rightleftharpoons (PbOH)_{ads} + e^- \quad [5]$$

$$(PbOH)_{ads} + OH^- \rightleftharpoons (PbO^-)_{ads} + H_2O \quad [6]$$

$$(PbO^-)_{ads} \rightleftharpoons PbO + e^- \quad [7]$$

Some dissolution of PbO was also found to occur during the nucleation and growth process, forming the $HPbO_2^-$ species (reaction [8])

$$PbO + OH^- \rightleftharpoons HPbO_2^- \quad [8]$$

In the work referred to above (13, 14), only the early stages of PbO film formation were examined. At more positive potentials in cyclic voltammetric experiments, or at longer times at constant potential, much thicker PbO films can be formed. It is the purpose of this paper to present the mechanism of the buildup of thick PbO films at Pb electrodes in *p*H 14 solutions. It will be shown here that these thick PbO films are very porous in nature, which is consistent with film initiation by a three-dimensional nucleation and growth process (14).

Experimental

The details of the electrochemical experiments, as well as the description of the cell, electrodes, and Pb electrode surface preparation, have been presented elsewhere (13, 14). In this work, all experiments were carried out at room temperature in 1*M* NaOH solutions, made from ACS Fisher grade NaOH and thrice-distilled water.

In the presentation of the data, the apparent electrode surface area (Pb disk, 0.38 cm^2) is utilized unless otherwise specified, and all potentials are given with respect to the RHE.

Curve simulations were done with the use of an IBM-PC, while the scanning electron microscope (SEM) investigations were carried out with a Cambridge Stereoscan 2500 SEM, equipped with a Kevex energy-dispersive x-ray analyzer.

Results and Discussion

Figure 1 shows a typical steady-state cyclic voltammogram (CV) for a Pb disk electrode in a 1*M* NaOH solution, obtained after a number of repeated cycles of potential. In

[1] Present address: Department of Geology and Geophysics, University of Calgary, Calgary, Alberta, Canada, T2N 1N4.

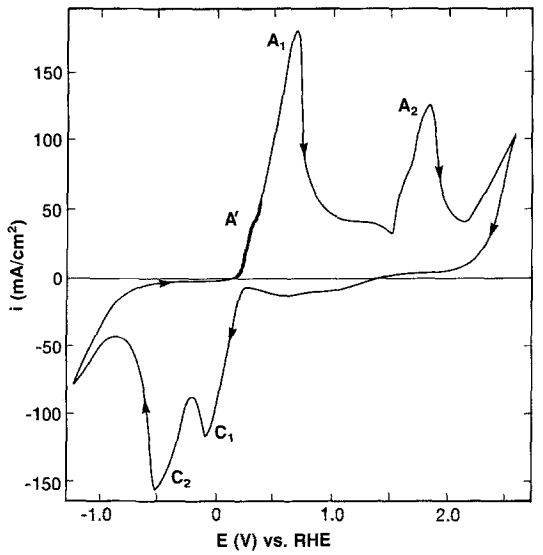

Fig. 1. General cyclic voltammetric response of Pb in 1M NaOH; s = 50 mV/s. The potential was extended between the range of hydrogen and oxygen evolution.

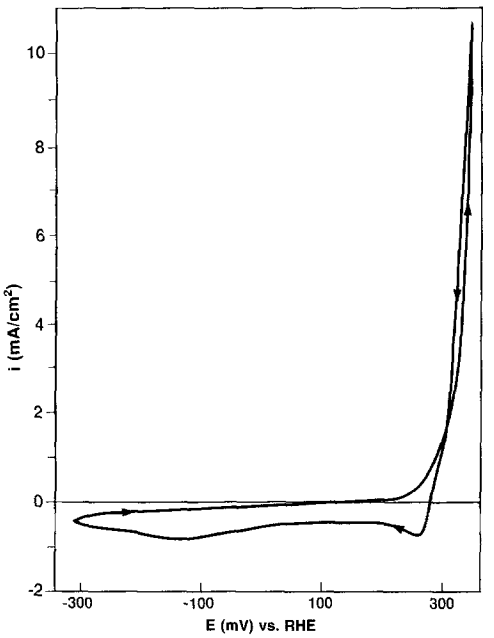

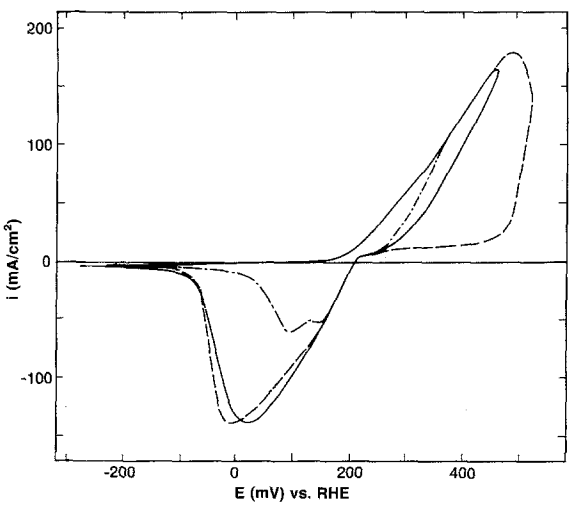

Fig. 2. (a) Anodic hysteresis in the early stages of Pb oxidation in 1M NaOH; s = 50 mV/s. (b) PbO formation and reduction when the upper potential limit is extended more positively with each cycle; s = 50 mV/s.

the anodic sweep, two principal peaks (A_1 and A_2) are observed. Based on thermodynamics, these are likely to represent PbO and PbO_2 film deposition, respectively. Peak C_1 has been found to be associated primarily with peak A_1 and therefore depicts the reduction of PbO to Pb, while peak C_2 reflects PbO_2 reduction. The anodic shoulder, A', has been shown to be related to $Pb(OH)_2$ deposition/dissolution (reactions [1]-[4]) (13), while the remaining anodic features, *e.g.*, the small peak and shoulder at 1.4 and 1.6V, respectively, remain unassigned, although they may be due to the formation of other Pb oxides such as Pb_2O_3 and Pb_3O_4 (13). Oxygen and hydrogen are evolved at the positive and negative limits, respectively, of the scan shown in Fig. 1.

It can be seen in Fig. 1 that the magnitude of the currents passed is very large, indicative of high rates of reaction of Pb in these alkaline solutions. Also, it can readily be seen that the anodic and cathodic charge densities are quite similar, showing that most of the oxidation products form as surface films which are then reduced in the cathodic scan. A more detailed examination of the charge densities shows that the anodic charges exceed the cathodic charges by a small amount, which is consistent with the involvement of some film dissolution at *p*H 14 (reactions [3] and [8]).

It was shown earlier that subsequent to the formation/dissolution of $Pb(OH)_2$ in shoulder A', another film process involving the nucleation and growth of PbO commences at potentials just positive of A' (14). Figure 2a shows an enlarged CV of the region at the foot of peak A_1. A type of hysteresis which is characteristic of film nucleation and growth is observed, *i.e.*, the oxidation current observed in the cathodic sweep is greater than that in the prior anodic sweep. When the potential is extended more positively (Fig. 2b), sufficient PbO film is deposited so that the hysteresis behavior of Fig. 2a is no longer seen.

The CV response obtained when the potential is extended over peaks A_1 and C_1 is displayed for several sweep rates (s) in Fig. 3. It can be seen that the leading slopes of peaks A_1 and C_1 are linear and constant at all s, indicative of an ohmically controlled reaction (IR compensation was not used in this work). The value of the reciprocal of this slope was found to be *ca.* 1.9Ω, which is very close to the value of the resistance of the solution, R_s, between the Pb disk surface and the tip of the Luggin capillary containing the reference electrode, as calculated by the Newman equation [Eq. [9], Ref. (15)]

$$R_s = (1/2\ \pi\kappa a)\ \tan^{-1}(d/a) \qquad [9]$$

where κ is the solution conductivity, d is the perpendicular distance from the tip of the Luggin capillary to the Pb disk surface, and a is the radius of the disk. In these experiments, a = 0.35 cm, d = *ca.* 1 cm, and κ = 0.18 S cm^{-1}.

An investigation of the relationship between the peak current density, $i_{p,A1}$, and the potential sweep rate is presented in Fig. 4 (— —). It can be seen that a linear relationship exists between $i_{p,A1}$ and $s^{1/2}$. An examination of the dependence of the peak potential, $E_{p,A1}$, on the sweep rate also yields a linear relationship between $E_{p,A1}$ and $s^{1/2}$ (Fig. 5).

The charge passed up to $E_{p,A1}$, measured by integration of the I/E response, has also been examined as a function of the sweep rate. A fairly constant value (*ca.* 2 C/cm^2) is observed, with the charges being somewhat larger at low s than at high s, and with an *ca.* 5-10% higher charge density observed in the anodic *vs.* the cathodic peaks. These observations are further evidence for PbO dissolution (reaction [8]) occurring along with PbO film deposition.

A model of film growth which is consistent with all of the observations described above concerning peak A_1 is that involving film formation at a rate controlled by both R_s and the resistance of the solution in pores, R_p, of a growing porous film (16). This, in turn, is based on Mueller's model (17) of film growth, which involves the initial random nucleation of small islands of film on the electrode surface. These nuclei are considered to form initially to a particular height, h, and then grow laterally until most of

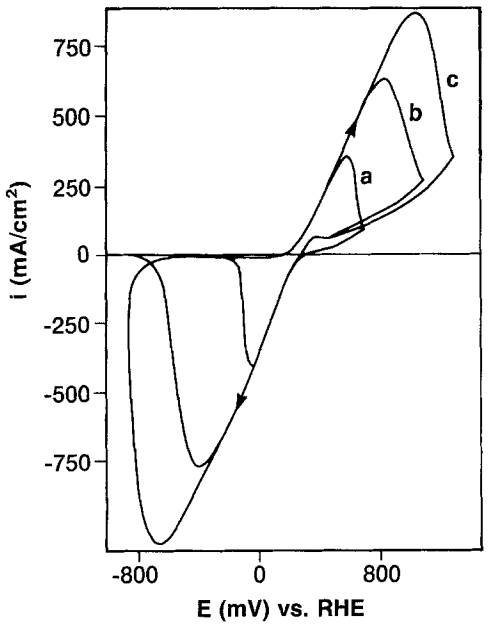

Fig. 3. *E/i* response of Pb in 1M NaOH at s = 50 mV/s (a), 200 mV/s (b), and 400 mV/s (c).

the electrode surface is covered, leaving only small pores between the adjacent islands of film.

Arvia (16) has considered the resistance of this film growth process as a function of electrode coverage. Initially, when only a few nuclei of film are present, only R_s controls the rate of the reaction. This is evidenced by the fact that the reciprocal of the leading side of peak A_1 is equivalent to the bulk solution resistance in the case of PbO film formation. However, as the nuclei spread, the pores between the growing islands of film become smaller. Assuming that the film growth reaction occurs by ion transfer to/from the metal/solution interface at the base of the pores, the increasing resistance of the narrowing pores of the film soon begins to control the reaction rate, causing it to decrease. This is the origin of the current peak and the drop in current after the peak, as seen in Fig. 3. This model of film growth, in which the growth rate depends on pore solution resistance, has also been found to hold in a number of other cases, *e.g.*, silver halide film growth at Ag electrodes (18, 19).

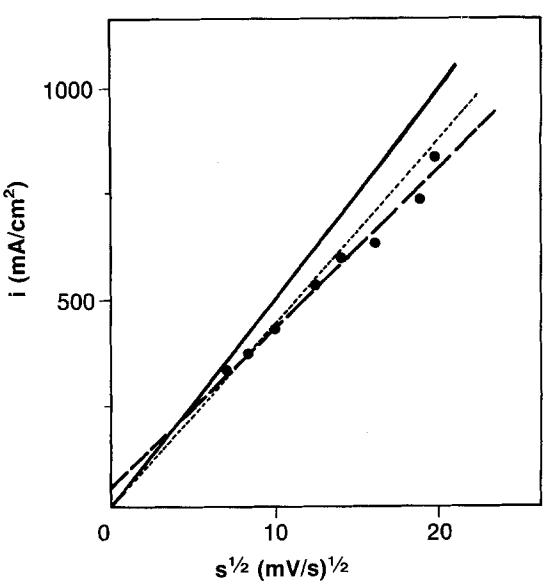

Fig. 4. Relationship between peak current densities of A_1 and $s^{1/2}$: experimental curves (--); calculated relationship from Eq. [15] for simple film spreading model (——); relationship obtained from differentiation of Eq. [20] for film spreading and thickening mechanism (----).

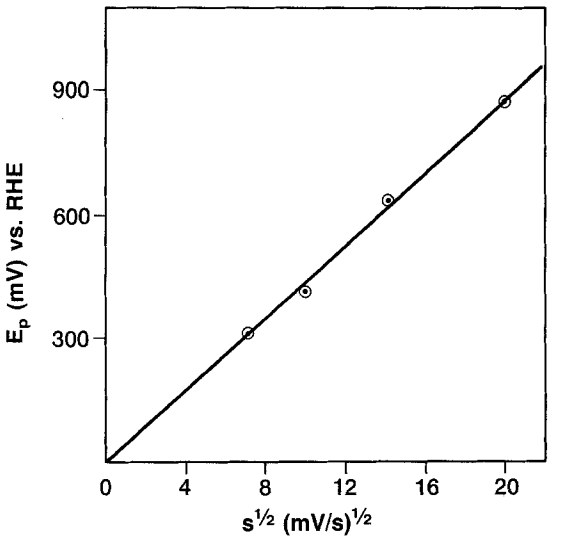

Fig. 5. Experimental relationship between peak potential of A_1 and $s^{1/2}$.

The resistance of the pores, R_p, can be described (16) according to Eq. [10]

$$R_p = h/[\kappa A(1 - \theta)] \quad [10]$$

Here, θ depicts the fraction of the Pb surface of apparent area, A, which is covered by the PbO film. Therefore, $A(1 - \theta)$ is equivalent to the free Pb surface area, *i.e.*, that area of the electrode still accessible to the reactant and not covered by PbO film.

When a reaction overpotential, η, is applied to the electrode, current will flow across the two resistors, R_s and R_p, according to Ohm's law

$$I = \eta/(R_s + R_p) \quad [11]$$

where

$$\eta = st \quad [12]$$

and s is the potential sweep rate. As the film grows laterally at a constant thickness, h, θ increases and Faraday's law can be used to convert the quantity of film formed to the amount of charge passed. The current can then be expressed as (16)

$$I = \frac{n\mathbf{F}\rho hA(d\theta/dt)}{M} = Q_m(d\theta/dt) \quad [13]$$

where n is the number of electrons passed per molecule of film material formed (= 2), ρ is the film density [9.5 g/cm^3 (20)], M is the film molecular weight [223.2 g/mol (20)], and **F** is the Faraday constant. Q_m is therefore the charge equivalent to full coverage of the electrode by a PbO film of thickness h.

If Eq. [10]-[13] are combined, then an expression for $d\theta/dt$ is obtained (16)

$$d\theta/dt = \frac{st}{Q_m\left[R_s + \dfrac{h}{\kappa A(1 - \theta)}\right]} \quad [14]$$

Equation [14] can be solved numerically for θ as a function of time by using an iterative process (16, 18, 19), *e.g.*, the Newton-Raphson method, commencing with an arbitrary, but small value of θ. The I/η relationship calculated as a function of time by this method can be compared with that observed experimentally to test the appropriateness of the pore resistance model of film growth for the PbO case.

Figure 6 shows a comparison of the i/η curves obtained by this method for four different sweep rates. $\eta = 0$ was taken as the potential at which the extrapolated leading slope of peak A_1 intercepts the potential axis. This was done because PbO film formation is actually preceded by

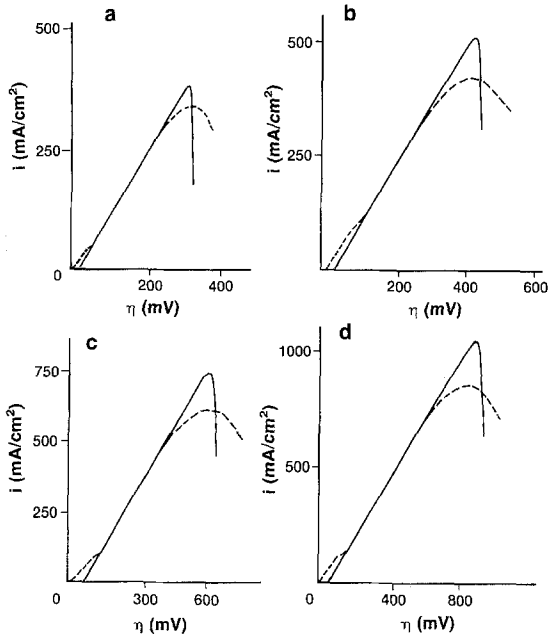

Fig. 6. Experimental (---) and calculated (——) I relationship for anodic PbO formation. $\eta = 0$ is defined at the extrapolated foot of peak A_1. The calculated curve is based on a porous film spreading mechanism (Eq. [13]). s = 50 (a), 100 (b), 200 (c), and 400 (d) mV/s.

the $Pb(OH)_2$ formation/dissolution process (shoulder A'), which is not considered to play a role in the pore resistance controlled growth of PbO film. It can be seen in Fig. 6 that both the calculated (——) and experimental (---) currents increase linearly toward the peak, with a reciprocal slope equal to R_s. However, the calculated curves have a very sharp peak, while the experimental curves are much more rounded. Also, in contrast to the calculated curves, the experimentally observed currents do not drop to zero immediately after the peak.

Another comparison of the experimental and calculated i/η relationship can be made by differentiation of Eq. [14] and determining the predicted dependence of i_p on s for this pore resistance model of film growth. This leads to Eq. [15], which reveals a linear relationship between i_p and $s^{1/2}$, as is also found experimentally

$$I_p/A = i_p = (n\mathbf{F}\kappa\rho/M)^{1/2}(1 - \theta)s^{1/2} \qquad [15]$$

Figure 4 shows the $i_p/s^{1/2}$ plot for the calculated curves (——) in comparison with the experimental (— —) results. Both plots are linear, but are not parallel. The degree of surface coverage by PbO at the current peaks, θ_p, can be calculated from the slope of the experimental plot by using Eq. [15]. Using the apparent electrode area of 0.38 cm^2, θ_p is found to be 0.966 by this method. If a relatively large roughness factor of the Pb electrode of *ca.* 5 is assumed, θ_p is 0.993. Using these θ_p values, an estimate of the PbO film thickness at the current peak can be made. If the apparent electrode surface area is again used in the calculation, h is *ca.* 590 nm, while if a reasonable roughness factor of 5 is assumed, h = *ca.* 120 nm.

The linear $E_p/s^{1/2}$ relationship shown in Fig. 5 is also consistent with the suggestion that the film pore resistance is the rate-determining step (16). This relationship can readily be derived from Eq. [11] and [15], if the peak parameters I_p and E_p are substituted for I and η.

Further support of this model of anodic film growth is obtained from an SEM analysis of the film morphology. Figure 7 shows a typical view of the electrode surface after oxidation in 1*M* NaOH solutions. In this case, the potential scan was terminated at the peak of A_1, revealing the very porous nature of the PbO film.

Overall, although the general shape and magnitude of the calculated and experimental current peaks are similar, there is only a fair fit between them, particularly in the region of the peak maxima. These results suggest that the

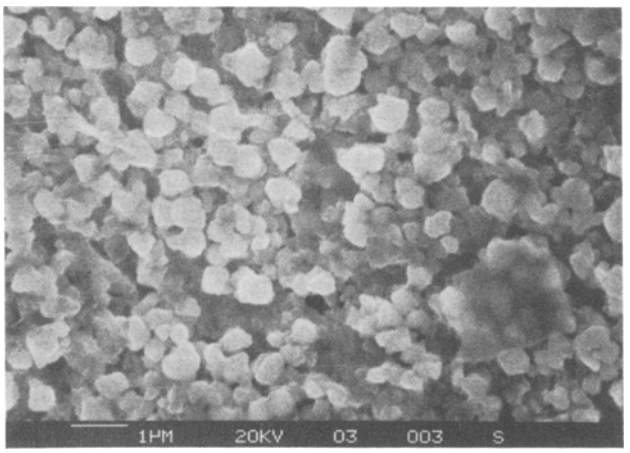

Fig. 7. SEM view of anodically formed PbO film. Potential sweep terminated at A_1 peak potential.

simple model of islands of film of constant height growing laterally on an electrode surface with increasing potential may not adequately describe the real film deposition process in the case of PbO. Therefore, the following modifications have been made to this simple model.

In order to improve the fit between the calculated and the experimentally observed i/η curves, it should first be recalled that the model used by Calandra *et al.* (16) assumes that the film thickness does not vary during the entire film growth process, at least up to the current peak. This model is not likely to be a very realistic representation of the growth of a thick and porous film. An alternative model for the growth of such a film has been presented by Birss and Wright (18). In this modified pore-resistance model of porous film growth, it has been assumed that the initial film nuclei grow in three dimensions with time, rather than in only two dimensions. Three-dimensional nucleation and growth is a more appropriate model for PbO film growth, as was shown earlier (14) by chronoamperometry.

In this modified model, the pores which develop between islands of film both narrow and lengthen with time. The current which flows can then be represented as being due to both film spreading and film thickening

$$I = Q'_m h d\theta/dt + Q'_m \theta dh/dt \qquad [16]$$

where Q'_m is equal to $n\mathbf{F}A\rho/M$. This equation contains two time-dependent variables, h and θ. As neither dh/dt nor $d\theta/dt$ are known, Eq. [16] cannot be solved exactly as a function of time.

Therefore, in order to obtain a simple expression for $d\theta/dt$, as was done above in Eq. [14], an arbitrary but reasonable dependence of h on time has been assumed (18), *i.e.*, it is assumed that the rate of film thickening, dh/dt, is directly proportional to the overpotential, η

$$dh/dt = j'\eta \qquad [17]$$

where j' is a film thickening rate constant obtained by a computer curve-fitting technique. Upon substitution of Eq. [17] into [16], followed by integration, an expression for h as a function of time is obtained

$$h = h_o + (j'/2)st^2 = h_o + jst^2 \qquad [18]$$

where h_o is the initial height of the nuclei when they are first deposited. The concept of the deposition of nuclei of PbO of constant height at very short times is consistent with the instantaneous nucleation model of film growth, found to apply in the case of PbO deposition at short times in response to a potential step (13). In order to determine I as a function of η, the values of the two arbitrary constants, j and h_o, must be established. This has been done by a best-fit calculation. By substituting Eq. [17] and [18] into Eq. [16], a time-dependent expression for the current is obtained.

$$I = Q'_m(h_o + jst^2)d\theta/dt + 2Q'_m\theta jst \qquad [19]$$

From this point on, the same approach is used to calculate the I/η relationship as was used for the simple pore resistance model described above. The current is again considered to be limited by R_s and R_p

$$I = R_s + \frac{st}{\{[h_o + jst^2]/[\kappa A(1 - \theta)]\}} \quad [20]$$

By combining Eq. [19] and [20], an expression for $d\theta/dt$ is obtained, analogous to that in Eq. [14]

$$d\theta/dt = \frac{st}{Q'_m h\left[R_s + \frac{(h_o + jst^2)}{\kappa A(1 - \theta)}\right]} - \frac{2j\theta st}{h} \quad [21]$$

The solution to this equation is again obtained by an iterative technique in which each small increment of time is recalculated from $d\theta/dt$ (Eq. [21]), h is incremented by the use of Eq. [17], and I is then determined at each θ (Eq. [20]). The calculations are carried out until θ is very large, and the calculated current becomes very small after the peak. By carrying out these calculations for various j and h_o values and using the apparent electrode area, the best fit for PbO film growth was obtained with the following values of j and h_o

$$j = 5 \times 10^{-8} \text{ cm/s/mV}$$

$$h_o = 80 \times 10^{-4} \text{ cm (800 nm)}$$

It should be noted that if the electrode roughness were known and could be taken into account, h_o would be smaller by this factor.

Figure 8 shows the comparisons of a number of experimental (----) and calculated (—) I/η curves for PbO film formation based on the modified pore resistance model described above. It can be seen that the fit between the two is quite good, with the calculated curves now being more rounded at the peak than in the case of the simple pore resistance model (Fig. 6). Also, the calculated currents do not drop to zero immediately after the current peak but rather decrease much more slowly, analogous to the experimental I/η curves. As a further test of the applicability of the modified pore resistance model of film growth to the PbO case, the calculated $i_p/s^{1/2}$ relationship based on the new model (----) is seen to display a closer fit to the experimental (— —) plot (Fig. 4) than does the data from the original pore resistance model (——).

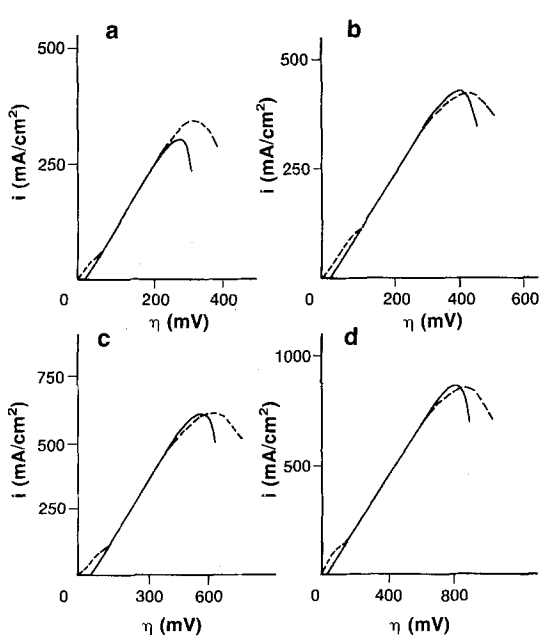

Fig. 8. Experimental (---) and calculated (——) i/η curves, based on film spreading and thickening model (Eq. [20]). s = 50 (a), 100 (b), 200 (c), and 400 (d) mV/s.

Overall, the modified pore resistance model, which allows for the film to thicken as well as to grow laterally with time until the electrode is essentially fully covered, produces a closer match with the experimental curves than does the simple film spreading model. The modified model also allows for a more natural progression from a nucleated surface film, to a thick, porous, anodically formed film.

Conclusions

This study has focused on the formation of thick PbO films at a Pb anode in pH 14 solutions. These films are known to initiate by an instantaneous three-dimensional nucleation process. SEM investigations have shown the films to be very porous. The current/voltage relationship, as seen by cyclic voltammetry, has been simulated on the basis of a model of film growth in which islands of PbO grow together, resulting in rate control by the increasing resistance of the solution in the pores of the film. Two models of island growth have been examined. The simple model of the lateral growth of PbO islands of constant height has led to a reasonable simulation of the observed results, although the calculated current peaks are too high and comparatively sharp. Significant improvement of the match between the experimental and calculated curves has been achieved by assuming that the nuclei both increase in height and spread laterally with increasing potential, or time, which is a much more realistic model of the growth of a porous film.

Acknowledgments

We are very grateful to the Natural Sciences and Engineering Council of Canada for financial support of this work.

Manuscript submitted Jan. 10, 1990; revised manuscript received April 6, 1990.

The University of Calgary assisted in meeting the publication costs of this article.

REFERENCES

1. S. R. Ellis, N. A. Hampson, M. C. Ball, and F. Wilkinson, *J. Appl. Electrochem.*, **16,** 159 (1986).
2. V. Danel and V. Plichon, *Electrochim. Acta,* **28(6),** 781, 785 (1983).
3. (a) G. Archdale and J. A. Harrison, *J. Electroanal. Chem. Interfacial Electrochem.*, **43,** 321 (1973); (b) *ibid.*, **47,** 93 (1973).
4. "Useful Information about Lead," 1st ed., Lead Industries Association, New York (1931).
5. W. Hoffman, "Lead and Lead Alloys," 2nd ed. Springer-Verlag, New York (1970).
6. K. Elbs and J. Forsell, *Zeit. Elektrochem.*, **8,** 760 (1902).
7. S. Glasstone, *J. Chem. Soc.*, **121,** 2091 (1922).
8. P. Jones, H. R. Thirsk, and W. F. K. Wynne-Jones, *Trans. Faraday Soc.*, **52,** 1003 (1956).
9. S. S. Popova and A. V. Fortunatov, *Sov. Electrochem.*, **2,** 413 (1966).
10. S. S. Popova and A. V. Fortunatov, *ibid.*, **2,** 626 (1966).
11. M. V. Ptitsyn, G. S. Zenin, and K. I. Tikhonov, *ibid.*, **13,** 1144 (1977).
12. L. M. Peter, *J. Electroanal. Chem. Interfacial Electrochem.*, **182,** 383 (1985).
13. V. I. Birss and M. T. Shevalier, *This Journal,* **134,** 802 (1987).
14. V. I. Birss and M. T. Shevalier, *ibid.*, **134,** 1594 (1987).
15. J. Newman, *ibid.*, **113,** 501 (1966).
16. A. J. Calandra, N. R. de Tacconi, R. Pereiro, and A. J. Arvia, *Electrochim. Acta,* **19,** 901 (1974).
17. W. J. Mueller, *Trans. Faraday Soc.*, **27,** 737 (1931).
18. V. I. Birss and G. A. Wright, *Electrochim. Acta,* **27,** 1429 (1982).
19. V. I. Birss and G. A. Wright, *ibid.*, **27,** 1439 (1982).
20. "CRC Handbook of Chemistry and Physics," 55th ed., CRC Press, Boca Raton, FL (1974-1975).
21. M. T. Shevalier, M. Sc. Thesis, University of Calgary, Calgary, Alb., Canada (1985).
22. H. Kieswetter and G. Moress, "Elementar Methoden der Numerischen," p. 95, Springer-Verlag, Berlin (1974).
23. C. R. Metz, "Schaum's Outline of Theory and Problems of Physical Chemistry," p. 4, McGraw-Hill, Toronto, Ont., Canada (1976).